Modelling the Functional Impact of KCNA5 Mutations on the Electrical and Mechanical Activities of Human Atrial Cells

Haibo Ni, Michael A Colman, Henggui Zhang

Biological Physics Group, the University of Manchester, Manchester, UK

Abstract

A recent study identified six mutations (three gain-of-function and three loss-of-function mutations) in the KCNA5 channel (encoding for the ultra-rapid delayed rectifier potassium current, I_{Kur}) associated with lone-atrial-fibrillation. However, the impact of the mutations on atrial electro-mechanical functions is unclear. In this study, we developed a coupled electro-mechanical model of the human atrial cell to investigate such functional impact. Our previously developed human atrial model was updated with a new I_{Kur} model, and was then coupled with the myofilament model proposed by Rice et al.. A stretch activated current was also incorporated to account for the mechanical feedback. Simulations of isometric and isotonic stretch conditions were performed to study the basic-cycle-length-adaptations of action potential duration and active force. It was shown that these mutations exhibited heterogeneous effects on human atrial electrical and mechanical activities. The gain-of-function mutations induced negative inotropic effects, whereas the loss-of-function mutations enhanced contractile functions. These results are in good agreement with a previous experimental study on effects of I_{Kur} block. In conclusion, the mutations significantly altered the adaptation properties of action potential and force, which could be pro-arrhythmic.

1. Introduction

Atrial fibrillation (AF) is the most common sustained cardiac arrhythmia in developed countries [1]. As being atrial-specific, I_{Kur} plays an key role in the repolarisation of human atrial myocytes [2]. Loss-of-function mutations in I_{Kur} have been linked with AF [3]. In a recent study, Christophersen *et al.* [2] identified six mutations in the KCNA5 channel associated with lone-AF, with variants of D322H, E48G and A305T resulting in gain-in-function of I_{Kur} and of D469E, Y155C and P488S resulting in loss-in-function. However, the impacts of these mutations on atrial electrical and mechanical functions are unclear. In this study, we developed a coupled electro-mechanical model of the human atrial cells to investigate the functional impacts of these mutations.

2. Methods

The human atrial cell model [1] and the myofilament model [4] were coupled to construct an electromechanical model for human atrial cells. Electro-mechanical feedback was introduced into the model via incorporating stretch-activated channels (SAC, and the current I_{SAC}). To simulate KCN5A mutations, the I_{Kur} model in the Colman *et al.* model [1] was updated to better describe the I-V relationship of wild type (WT) and KCN5A mutations observed experimentally, as shown in Figure 1.

The Rice *et al.* model [4] was also updated to better approximate the Ca^{2+}-tension relationship observed experimentally at 20 °C [5] (Figure 2A), with minor modifications to the transition rates in the model. Q_{10} correction was adopted to simulate the active force at physiological temperature. Figure 2B shows the dependence of force activation on sarcomere lengths. In the simulations, the Ca^{2+}-tension relationship and SAC were assumed to be not affected by the mutations.

Based on a previous study [6], I_{SAC} was incorporated into the model using the following formulation:

$$I_{SAC} = G_{stretch} \cdot P_m \cdot (V_m - E_{stretch}) \quad (1)$$

where $G_{stretch}$ and $E_{stretch}$ are the maximum conductance and reversal potential of the channel, V_m the membrane potential, and P_m the normalised open probability of I_{SAC}, which has been described in detail elsewhere [6]. I_{SAC} was assumed to be permeable to three major ions: Na^+, K^+ and Ca^{2+}, considering two permeability ratios (P_{Na}:P_K:P_{Ca} = 1:1:0 and 1:1:1 [6], where P_{Na}, P_K and P_{Ca} are the relative permeabilities of SAC to the corresponding ion.)

Isometric and isotonic stretch protocols (ISOM and ISOT) were considered to compute the active force. In both protocols, the initial sarcomere length (SL) was set to 2.2 μm. Dynamic restitution properties of APD_{90} (action potential duration at 90% repolarisation) and the maximum active force were simulated. For each basic cycle length (BCL), a train of 100 stimuli was applied, and the last 30 beats were recorded for analysis. The

amplitude of alternans in APD_{90} was quantified by finding the maximum difference in APD_{90} between two successive action potentials (APs). The windows of BCL giving rise to alternans or irregular APs were measured.

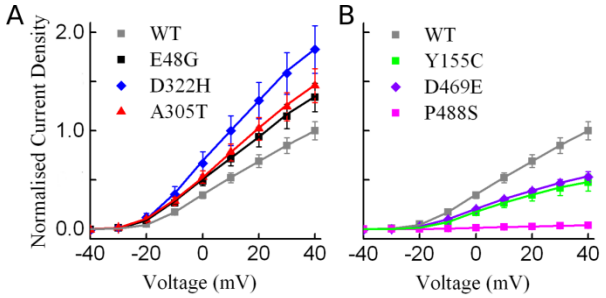

Figure 1. Experimental and simulated I-V relationships of I_{Kur} for gain-in-function mutations (A) and loss-in-function-mutations (B). Symbol with error bars: experimental data [2]. Line: simulation data.

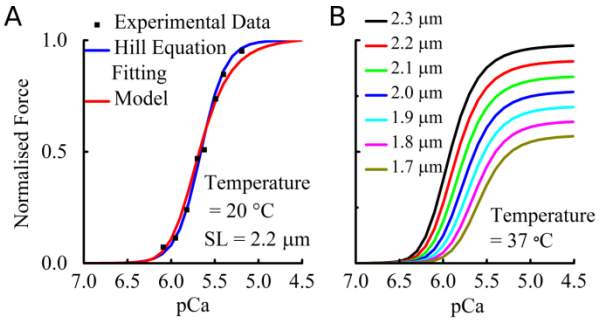

Figure 2. Simulated Ca^{2+}-tension relationships (line) as compared to experimental data (symbol) [5]. (A) The Ca^{2+}-tension relationship; the active forces were normalised to the force at pCa ($-\log_{10}[Ca^{2+}]$) = 4.5. (B) Simulated active forces with variant SLs. The forces were normalised to the maximum force of the cell in the model.

3. Results

The coupled electro-mechanical model faithfully reproduced the characteristics of AP and active force traces, as shown in left panels of Figure 3 and 4. Larger forces were elicited in isometric condition due to higher force sensitivity to Ca^{2+} at SL = 2.2 µm. A maximum cell shortening of 7.9% was observed under WT condition.

All mutations demonstrated marked effects on the electrical properties and active forces, as well as their adaptations to BCLs. Effects of variant E48G and A305T on AP and force were closely similar to each other, and so did Y155C and D469E. Therefore, only results from mutations A305T and D469E are shown here.

3.1. Effects on action potentials and force

Effects of the mutations and incorporation of I_{SAC} on APs, intracellular Ca^{2+} ($[Ca^{2+}]_i$) and active forces were shown in Figure 3 (ISOM simulations) and Figure 4 (ISOT simulations). A summary is shown in Figure 5. Active forces were normalised to the maximum values of the corresponding WT.

The loss-of-function mutations significantly elevated the plateau potential, increased APD at 30% and 50% repolarisation (APD_{30} and APD_{50}), prolonged APD_{90} and increased the systolic $[Ca^{2+}]_i$, leading to profound augmentation in the active force and cell length shortening, especially for the mutant P488S, which nearly abolished I_{Kur}. These simulation results are consistent with a previous experimental study [7], showing that blocking I_{Kur} increased systolic $[Ca^{2+}]_i$, force and cell length shortening in atrial cells.

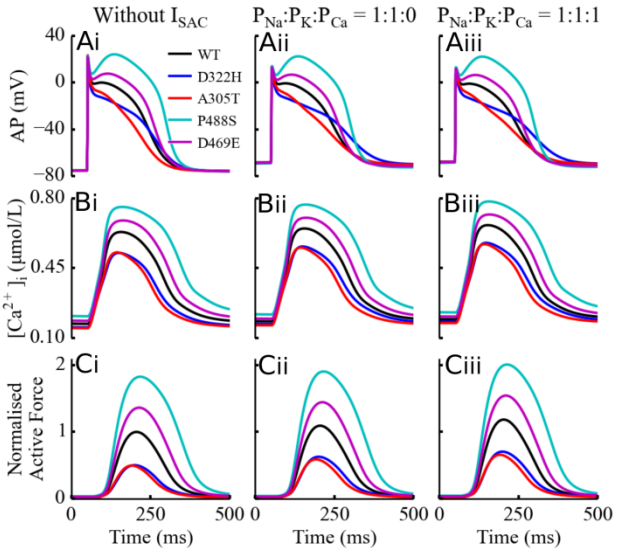

Figure 3. Effects of KCNA5 mutations and I_{SAC} on AP (Ai-Aiii), $[Ca^{2+}]_i$ (Bi-Biii), and maximum active force (Ci-Ciii) in ISOM conditions. BCL = 1000 ms.

The gain-of-function mutations elicited more negative plateau potential and thus significantly reduced APD_{30} and APD_{50}. E48G and A305T reduced APD_{90}, whereas D322H the variant with most profound increase of I_{Kur} current density, prolonged APD_{90}. All the gain-of-function mutations showed markedly reduced systolic $[Ca^{2+}]_i$ and thus significantly decreased force and shortening, demonstrating negative inotropic effects.

In the absence of I_{SAC}, ISOM and ISOT simulations produced similar results. Inclusion of I_{SAC} depolarised the resting potential (from -76 mV to -71 mV under WT, and similar change was observed with mutations). In the ISOM simulations, inclusion of I_{SAC} prolonged APD_{90} of the WT and more profoundly in the gain-of-function variants, whereas the APD_{90} was mildly reduced in the loss-of-function mutations. In the ISOT simulations, APD_{90} was abbreviated in the presence of I_{SAC}. The inclusion of permeability of I_{SAC} to Ca^{2+} ($P_{Na}:P_K:P_{Ca}$ =

1:1:1) slightly augmented systolic $[Ca^{2+}]_i$ and promoted contractile function without significantly changing APD_{90}.

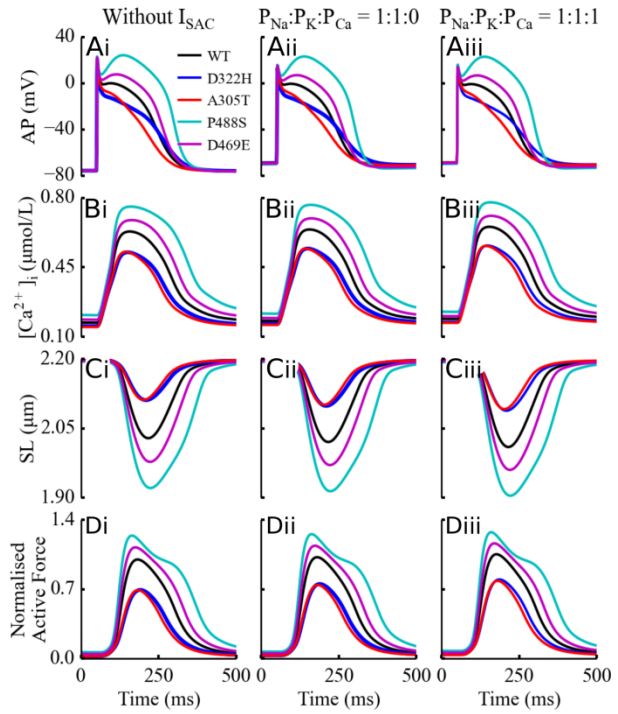

Figure 4. Effects of KCNA5 mutations and I_{SAC} on AP (Ai-Aiii), $[Ca^{2+}]_i$ (Bi-Biii), SL (Ci-Ciii) and active force (Di-Diii) in ISOT conditions. BCL = 1000 ms.

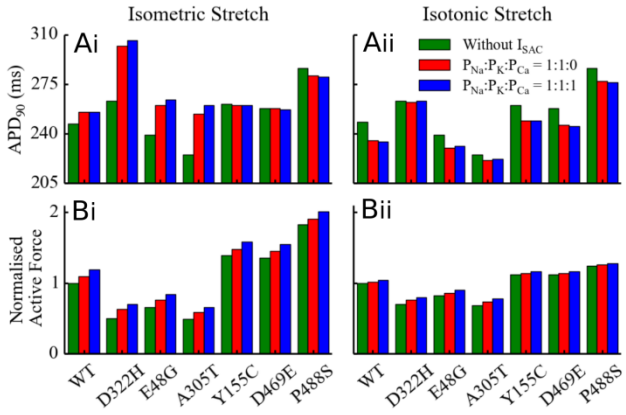

Figure 5. Summary of effects of KCNA5 mutations and inclusion of I_{SAC} on APD_{90} (Ai-Aii) and normalised active force (Bi-Bii) under ISOM and ISOT conditions.

3.2. Effects on the APD and force adaptations to BCL

Effects of mutations and I_{SAC} on the dynamic restitutions of APD and maximum active force are shown in Figure 6. Mutations of E48G and A305T flattened the adaptation curve, whereas D322H and the loss-of-function mutants steepened the curve. In the presence of I_{SAC}, APD_{90} was slightly reduced at BCLs higher than 700 ms with the gain-of-function mutations, whereas the same effect was not observed with the loss-of-function variants.

The maximum active force-BCL relationship is qualitatively comparable to experimental data of human ventricular cells [8], with the curve peaking in a range of BCLs between 650 ms and 850 ms. The loss-in-function mutations significantly increased the BCL-adaptation of maximum force, whereas the force restitution curves were profoundly flattened under gain-of-function conditions, showing significant reduction in adaptations to BCLs.

In the absence of I_{SAC}, P488S showed the largest amplitude in APD_{90} alternans (50 ms), whereas amplitudes around 20 ms were seen in WT and the rest mutations. In the presence of I_{SAC}, the amplitude was almost doubled in the ISOM simulations, and significantly decreased in the ISOT simulations, except for P488S, due to a marked increase in the effective refractory period (ERP).

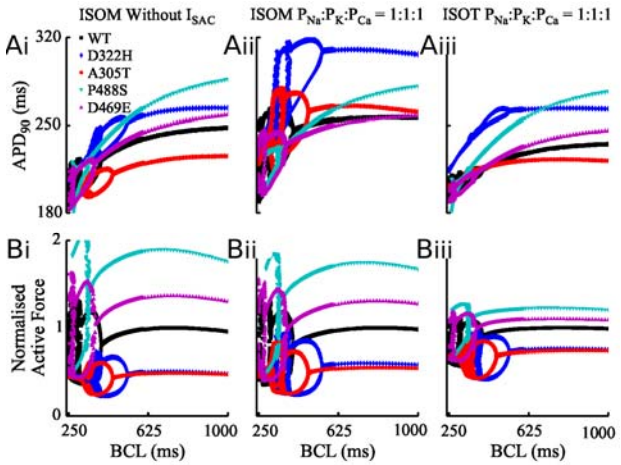

Figure 6. Effects of mutations and I_{SAC} on the APD_{90} (Ai-Aiii) and maximum force BCL-adaptations (Bi-Biii). (Ai-Bi) without I_{SAC}; (Aii-Bii) ISOM and (Aiii-Biii) ISOT conditions with I_{SAC}. $P_{Na}:P_K:P_{Ca}$ = 1:1:1. Smaller BCL steps were utilised for BCLs between 250 ms and 600 ms.

Beat-to-beat variations in AP were observed in simulations with BCLs in a range between 250 ms and 500 ms, which was accompanied by beat-to-beat variations in the active force. The BCLs eliciting these variations were characterised by a window generating typical alternans (W_A), and a window resulting in irregular AP and force variations (W_{IV}). The amplitudes of APD_{90} alternans were summarised in Figure 7A, and the two windows (W_A and W_{IV}) are shown in Figure 7B. W_A and W_{IV} were significantly positively shifted by the gain-of-function mutants, increasing the vulnerability to alternans. D322H also induced a marked increase in the range of W_A. The windows were moderately negatively shifted by the loss-of-function mutants. The mutation P488S with longest APDs showed typical alternans for

BCLs between 270 ms and 350 ms, and fell into the ERP for even smaller BCLs. Inclusion of I_{SAC} increased the range of W_A for the gain-of-function mutations in ISOM simulations, whereas the ranges of W_A were reduced by mutations of E48G and A305T. The ranges of W_A were not affected by the simulation conditions or I_{SAC} in the loss-of-function mutations.

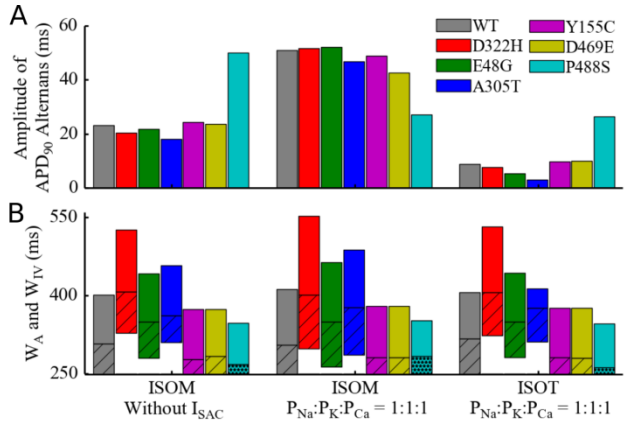

Figure 7. Amplitude and window of BCL for alternans and irregular APs. (A) Amplitude of APD_{90} alternans; (B) W_A and W_{IV}. Diagonal hatched bars show the W_{IV} and the dotted ones indicate the window of ERP.

4. Discussion and conclusion

An electromechanical coupled model for simulating the electrical and mechanical activities of human atrial cells was developed in the present study. This model allows *in-silico* investigation of arrhythmogenesis of AF, including the functional impacts of genetic variations.

Our simulations demonstrated that the KCNA5 mutations have marked effects on the electrical and mechanical functions of human atrial cells. The gain-of-function of the KCN5A mutations generates more negative plateau potentials of AP, results in reduced active forces. The loss-of-function of the KCN5A mutations prolongs APD_{90}, elevates the plateau potentials of AP and systolic $[Ca^{2+}]_i$, showing positive inotropic effects. These simulation results match to experimental data [7], and support the theory of modulation of contractility by the shape of AP, especially the plateau potentials in the atrial cells [7].

The simulation results also showed that the BCL-adaptations of APD and maximum force were altered by the mutations. Two gain-of-function variants (E48G and A305T) flattened the APD restitution curve and thus potentially increased the vulnerability to AF [9], whereas D322H and the loss-of-function mutants steepened the APD restitution curve. The force BCL-adaptations were significantly reduced by the gain-of-function mutations, whereas they are markedly enhanced by the loss-of-function mutations. Typical alternans and irregular beat-to-beat variations were observed in the simulations. Gain-of-function mutations are more prone to alternans.

Furthermore, it was demonstrated that I_{SAC} played an important role in modulating the APs and active forces. Inclusion of I_{SAC} showed positive inotropic effects, which is consistent with previous simulation study [6].

Acknowledgements

This work was supported by a project grant from EPSRC UK (EP/J00968X/1).

References

[1] Colman MA, Aslanidi OV, Kharche S, Boyett MR, Garratt C, Hancox JC, et al. Pro-arrhythmogenic effects of atrial fibrillation-induced electrical remodelling: insights from the three-dimensional virtual human atria. J Physiol 2013;591:4249–72.

[2] Christophersen IE, Olesen MS, Liang B, et al. Genetic variation in KCNA5: impact on the atrial-specific potassium current IKur in patients with lone atrial fibrillation. Eur Heart J 2013;34:1517–25.

[3] Olson TM, Alekseev AE, Liu XK, Park S, Zingman LV, Bienengraeber M, et al. Kv1.5 channelopathy due to KCNA5 loss-of-function mutation causes human atrial fibrillation. Hum Mol Genet 2006;15:2185–91.

[4] Rice JJ, Wang F, Bers DM, de Tombe PP. Approximate Model of Cooperative Activation and Crossbridge Cycling in Cardiac Muscle Using Ordinary Differential Equations. Biophys J 2008;95:2368–90.

[5] Narolska NA, Eiras S, Loon RB van, et al. Myosin heavy chain composition and the economy of contraction in healthy and diseased human myocardium. J Muscle Res Cell Motil 2005;26:39–48.

[6] Adeniran I, Hancox JC, Zhang H. In silico investigation of the short QT syndrome, using human ventricle models incorporating electromechanical coupling. Front Card Electrophysiol 2013;4:166.

[7] Schotten U, Haan S de, Verheule S, Harks EGA, Frechen D, Bodewig E, et al. Blockade of atrial-specific K^+-currents increases atrial but not ventricular contractility by enhancing reverse mode Na^+/Ca^{2+}-exchange. Cardiovasc Res 2007;73:37–47.

[8] Mulieri LA, Hasenfuss G, Leavitt B, Allen PD, Alpert NR. Altered myocardial force-frequency relation in human heart failure. Circulation 1992;85:1743–50.

[9] Kneller J, Sun H, Leblanc N, Nattel S. Remodeling of Ca^{2+}-handling by atrial tachycardia: evidence for a role in loss of rate-adaptation. Cardiovasc Res 2002;54:416–26.

Address for correspondence.

Haibo Ni.
Room 3.17, Schuster Building,
The Univerisity of Manchester,
Manchester, UK,
M13 9PL.
haibo.ni@postgrad.manchester.ac.uk